# Pressure-Induced Freezing of the Hydrophobic Core Leads to a L $1 \rightarrow$ H $1$ Phase Transition for C $12$ E $5$ Micelles in D $2$ O

4 AUTHORS, INCLUDING:

Dobrin P Bossev
Indiana University Bloomington
20 PUBLICATIONS 264 CITATIONS

SEE PROFILE

Michael Paulaitis
Johns Hopkins Medicine
165 PUBLICATIONS 4,718 CITATIONS

SEE PROFILE

# Pressure-Induced Freezing of the Hydrophobic Core Leads to a $L_1 \rightarrow H_1$ Phase Transition for $C_{12}E_5$ Micelles in $D_2O$

D. P. Bossev,[†] S. R. Kline,[§] J. N. Israelachvili,[‡] and M. E. Paulaitis*,[†]

*Department of Chemical Engineering, Johns Hopkins University, Baltimore, Maryland 21228-2694, National Institute of Standards & Technology, Center for Neutron Research, Gaithersburg, Maryland 20899-8562, and Department of Chemical Engineering and Materials Research Laboratory, University of California at Santa Barbara, Santa Barbara, California 93106*

We apply small-angle neutron scattering (SANS) to study the effect of pressure on micelle structure in a solution of 1% by weight pentaethylene glycol mono-*n*-dodecyl ether ($C_{12}E_5$) in $D_2O$ at 20 °C and pressures up to ~3000 bar. At ambient pressure, the structure is a network of branched, semiflexible, cylindrical micelles with the branch points comprised of three-armed junctions. Our SANS results reveal that pressure induces a phase transition from this network of threadlike micelles to hexagonally ordered bundles of cylindrical micelles. Using geometric packing constraints for three-arm junctions and cylinders, we show that the formation of three-arm junctions becomes increasingly unfavorable with increasing pressure due to the compression of the micelle hydrophobic core, and as such, the network becomes unstable at pressures close to those observed in our SANS experiments. We also measured the temperature dependence of the transition pressure and find that it follows the pressure−temperature freezing curves for liquid *n*-alkanes of comparable hydrocarbon chain length. These observations lead us to propose that the phase transition is related to a loss of flexibility or conformational entropy of the $C_{12}E_5$ micelles upon the pressure-induced freezing of the micelle hydrophobic core to form an amorphous solid. The formation of hexagonally ordered bundles of cylindrical micelles follows as attractive van der Waals forces between the micelles are not offset by the loss of repulsive undulation forces arising from the fluidity of the hydrophobic core.

## Introduction

Nonionic surfactants of the type $C_iE_j$ (*n*-alkyl polyoxyethylene ether) form a variety of microstructures in water, ranging from simple micelles at low surfactant concentrations to complex mesophases, such as hexagonal or lamellar phases, at high concentrations.[1,2] These microstructures have been studied as a function of temperature, the hydrophobic−lipophobic balance of the amphiphile, the addition of alkanes, and the addition of salts or ionic cosurfactants. The effect of pressure on the structure of micelles and microemulsions, however, has not been studied as extensively. In general, small angle neutron scattering (SANS) is particularly well suited for such measurements because the range of length scales probed includes both the particle size and the interparticle spacing. Pressure effects observed in high-pressure SANS measurements of surfactant microstructure[3−6] are typically interpreted by invoking geometric packing arguments that focus on the more compressible oil phase or hydrophobic tails of the surfactant.[7,8] In this context, increasing pressure destabilizes contact configurations between the hydrophobic tails at the oil−water interface relative to solvent-separated configurations,[9] thereby increasing the curvature of the oil−water interface.[10] Conversely, increasing temperature decreases the curvature of the oil−water interface. The underlying mechanism for this temperature dependence is thought to be the dehydration of the nonionic headgroups with increasing temperature, which leads to more efficient headgroup packing.[11] Thus, temperature and pressure can be viewed as thermodynamic variables which influence the microstructure of nonionic surfactant microemulsions and micellar solutions through inherently different molecular mechanisms.

In this Letter, we report the results of high-pressure SANS experiments on a solution of 1 wt % pentaethylene glycol mono-*n*-dodecyl ether ($C_{12}E_5$) in $D_2O$ at 20 °C and pressures up to ~3000 bar. The phase diagram for this system at ambient pressure is shown in Figure 1. At this temperature and surfactant concentration, a single-phase micellar solution ($L_1$ phase) forms at ambient pressure, well below the lower critical solution temperature (LCST) for liquid−liquid equilibrium and far removed from the $H_1$ hexagonal phase at much higher $C_{12}E_5$ concentrations. The application of pressure shifts the LCST to higher

[†] Department of Chemical Engineering, Johns Hopkins University.

[§] National Institute of Standards & Technology, Center for Neutron Research.

[‡] Department of Chemical Engineering and Materials Research Laboratory, University of California at Santa Barbara.

(1) Strey, R. *Ber. Bunsen-Ges. Phys. Chem.* **1996**, *100*, 182.

(2) Strey, R.; Schomäcker, R.; Roux, D.; Nallet, F.; Olsson, U. *J. Chem. Soc., Faraday Trans.* **1990**, *86*, 2253.

(3) Gorski, N.; Kalus, J.; Schwahn, D. *Langmuir* **1999**, *15*, 8080 and references therein.

(4) Steytler, D. C.; Holmes, J. D. *Current Opin. Colloid Interface Sci.* **1998**, *3*, 299 and references therein.

(5) Nagao, M.; Seto, H. *Phys. Rev E* **1999**, *59*, 3169 and references therein.

(6) Eastoe, J.; Steytler, D. C.; Robinson, B. H.; Heenan, R. K. *J. Chem. Soc., Faraday Trans. 1* **1994**, *90*, 3121 1994 and references therein.

(7) Nagao, M.; Okuhara, D.; Seto, H.; Komura, S.; Takeda, T. *Jpn. J. Appl. Phys., Part 1* **1999**, *38*, 951.

(8) Israelachvili, J. N.; Mitchell, D. J.; Ninham, B. W. *J. Chem. Soc., Faraday Trans. 1* **1976**, *72*, 1525.

(9) Hummer, G.; Garde, S.; García A. E.; Paulaitis, M. E.; Pratt, L. R. *Proc. Natl. Acad. Sci. U.S.A.* **1998**, *95*, 1552.

(10) Positive interfacial curvature is defined with respect to the oil phase or the hydrophobic micelle core.

(11) Strey, R. *Colloid Polym. Sci.* **1994**, *272*, 1005.
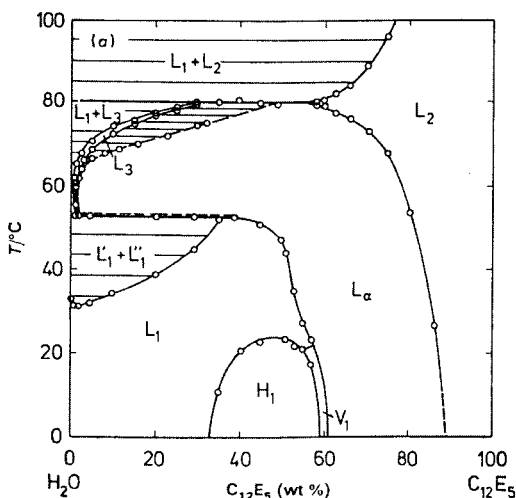
**Figure 1.** Temperature−composition phase diagram for $C_{12}E_5$/water solutions at ambient pressures. Data were obtained from: Strey, R.; Schomäcker, R.; Roux, D.; Nallet, F.; Olsson, U. *J. Chem. Soc., Faraday Trans.* **1990**, *86*, 2253.



**Figure 2.** Measured SANS spectra at 20 °C for 1 wt % $C_{12}E_5$ in $D_2O$ as a function of pressure and 49 wt % $C_{12}E_5$ in $D_2O$ at ambient pressure.

temperatures.[12] The effect of pressure on the $H_1$ phase is not known. The microstructure of the $L_1$ phase at 1 wt % $C_{12}E_5$, 20 °C, and ambient pressure is a network of branched, semiflexible, cylindrical micelles with the branch points comprised of three-armed junctions.[13−16] Our SANS results reveal that pressure induces a transition from this network of threadlike micelles to hexagonally ordered bundles of cylindrical micelles. An analysis of the geometric packing constraints for three-arm junctions and cylinders shows that this network becomes unstable at a pressure close to that observed in our SANS experiments. We also measured the temperature dependence of the transition pressure and find that the $p-T$ curve follows the $p-T$ freezing curves for liquid *n*-alkanes of comparable hydrocarbon chain length. On the basis of this finding, we hypothesize that the transition is related to a pressure-induced loss of flexibility or conformational entropy of the $C_{12}E_5$ micelles upon freezing of the micelle hydrophobic core to form an amorphous solid.

## Experimental Section

Scattering experiments were performed on the NG3 30-m SANS instrument at the NIST Center for Neutron Research in Gaithersburg, MD. Neutrons of wavelength $\lambda = 6$ Å with a distribution of $\Delta\lambda/\lambda = 15\%$ were incident on samples held in a custom-built high-pressure SANS cell. A single sample-to-detector distance of 315 cm was used to give a $q$-range of 0.0122 $Å^{-1} < q < 0.2208$ $Å^{-1}$, where $q = (4\pi/\lambda)\sin(\theta/2)$ is the magnitude of the scattering vector. Sample scattering was corrected for background and empty cell scattering, and the sensitivity of individual detector pixels was normalized. Corrected data sets were circularly averaged and placed on an absolute scale using standard samples and software supplied by NIST.[17] Instrumental smearing was simulated[18] for the instrument configurations used, eliminating smeared data points from the combined data set.

(12) Nishikido, N.; Yoshimura, N.; Tanaka, M.; Kaneshina, S. *J. Colloid Interface Sci.* **1980**, *78*, 338.

(13) Bernheim-Groswasser, A.; Watchel, E.; Talmon, Y. *Langmuir* **2000**, *16*, 4131.

(14) The existence of three-arm junctions as the branch points in such networks, proposed earlier on theoretical grounds,[15,16] was confirmed by these direct cryo-TEM microscopy observations.

(15) Drye, T. J.; Cates, M. E. *J. Phys. Chem.* **1992**, *96*, 1367.

(16) Bohbot, Y.; Ben-Shaul, A.; Granek, R.; Gelbart, W. M. *J. Chem. Phys.* **1995**, *103*, 8764.

(17) NIST SANS Data Reduction and Imaging Software, 1998.

(18) Barker, J. G.; Pedersen, J. S. *J. Appl. Crystallogr.* **1995**, *28*, 105.
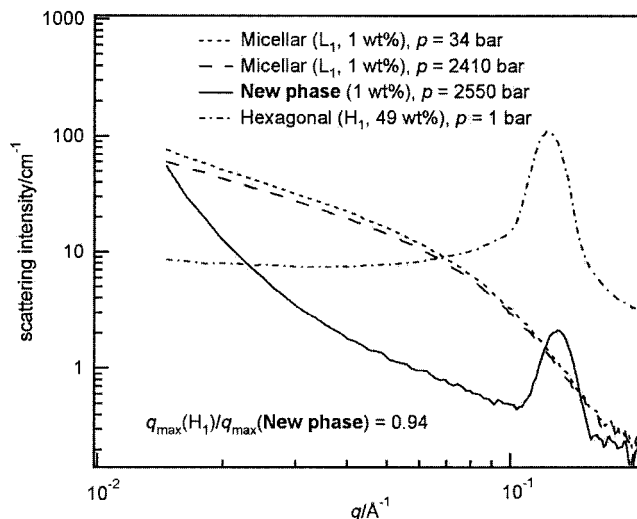
The custom-built high-pressure SANS cell consists of a stainless steel outer cell, rated to 4 kbar, and an inner cell containing the surfactant solution. The design of this high-pressure cell is described in detail elsewhere.[19] A unique feature of the cell design is to isolate the sample from the pressurizing fluid and the metal walls of the outer cell by enclosing it in the inner cell. This inner cell consists of a flexible Teflon sleeve that fits tightly around the two sapphire windows of the outer cell such that the sample path length (i.e., the distance between the windows) is 1.00 mm at atmospheric pressure. The change in path length due to deformation of the high-pressure cell at kilobar pressures was accounted for based on an independent calibration of this correction.[19]

Temperature was controlled using a constant-temperature bath provided by NIST (±0.01 °C sensitivity) which circulated ethylene glycol through the aluminum jacket that held the high-pressure cell. Temperature was measured with an Omega E-type thermocouple and meter (±0.5 °C accuracy). The stability of the temperature readings during an experiment was ±0.1 °C. Pressure was generated and controlled manually using a pressure generator, and measured at the cell using a Viatran model 345 transducer (0−60000 psi, ≤±60 psi nonlinearity) and meter (±1 psi sensitivity).

$C_{12}E_5$ (>98% purity) was purchased from Nikko Chemicals and used without further purification. $D_2O$ (99.9% purity) was purchased from Aldrich Chemicals. The surfactant was apportioned into 2.5 mL aliquots in a glovebox and then stored at −15 °C until used. Solutions of 1 wt % $C_{12}E_5$ in $D_2O$ were prepared by weight and allowed to equilibrate overnight at room temperature.

## Results and Discussion

The scattering curves obtained at 34, 2410, and 2550 bar are shown in Figure 2. The curves at 34 and 2410 bar are virtually identical, indicating no significant change in microstructure with increasing pressure up to 2410 bar. Fitting these curves using a form factor for cylindrical micelles[20] gives a radius of $21.0 \pm 0.2$ Å and a length greater than 600 Å, independent of pressure.[21] However, a small increase in pressure from 2410 to 2550 bar leads to the appearance of a peak in the scattering intensity at $q \sim 0.130$ $Å^{-1}$, indicative of a highly ordered system. Visual

(19) Ferdinand, S. Pressure-Induced Changes in Microstructure of Oil-In−Water Microemulsions, M.S. Thesis, Johns Hopkins University, 2000.

(20) Guinier, A.; Fournet, G. *Small Angle Scattering of X-rays*; John Wiley & Sons: New York, 1955.

(21) The maximum length that could be resolved (∼600 Å) was limited by the minimum $q$-value measured.

observations confirmed a completely reversible transition from a transparent solution at 2410 bar to an opaque solution at 2550 bar. This transition was also observed in the SANS spectra at lower temperatures and correspondingly lower pressures (data not shown). The identical transition has been reported by others in SANS studies of tetradecyldimethylaminoxide (TDMAO) micelles in $D_2O$ at pressures up to 3000 bar.[3,22] A determination of the microstructure in the new high-pressure phase was not attempted, although a lamellar structure was conjectured.

Also shown in Figure 2 is the scattering curve for the $H_1$ hexagonal phase at 49 wt % $C_{12}E_5$, 20 °C, and ambient pressure. The peak at $q \sim 0.120$ Å$^{-1}$ that arises from the hexagonal lattice of cylindrical micelles[23] is similar to the one for the 1 wt % $C_{12}E_5$ solution at 2550 bar, suggesting that this new high-pressure phase may resemble a slightly compressed state of the $H_1$ hexagonal phase at ambient pressure. A similar scattering curve with a peak at $q \sim 0.150$ Å$^{-1}$ was obtained for the $L_\alpha$ lamellar phase at 79 wt % $C_{12}E_5$, 20 °C, and ambient pressure (data not shown). However, the formation of planar bilayers from cylindrical micelles corresponds to increasing the hydrophobic core volume-to-surface-area ratio per surfactant molecule or, equivalently, decreasing the spontaneous curvature of the surfactant film,[8,24] and the application of pressure would have the opposite effect. We conclude, therefore, that the observed change in microstructure corresponds to a pressure-induced $L_1 \rightarrow H_1$ phase transition from a network of branched, semiflexible, cylindrical micelles to hexagonally ordered bundles of cylindrical micelles.

The effect of pressure on the stability of the $L_1$-phase network can be evaluated based on geometric packing constraints for the hydrocarbon chains of surfactant molecules forming the branch points (three-arm junctions) and the cylinders using the following dimensionless parameter[8]

$$\eta \equiv v/a_0 l_c \tag{1}$$

where $v$ is the hydrophobic core volume per surfactant molecule, $a_0$ is the optimum surface area per surfactant molecule at the hydrocarbon−water interface, and $l_c$ is a critical length less than or equal to the fully extended hydrocarbon chain of the surfactant. For the three-arm junction model shown in Figure 3, these constraints separate into those that apply within the cylindrical regions and those that apply at the junction. The two regions are bounded by circular cross sections that project to the triangle ABC shown in the top drawing. Although this topological model is not unique, it does satisfy the main packing constraint that no internal part of the junction is farther away from the surface than $l_c$, given that $r \approx l_c$. The lower drawing shows how each cylinder is sectioned at the junction. The cylindrically shaded region ABD (one on either side) is the exposed surface of area $A$ occupied by the surfactant headgroups, and the two-sided pyramid ABD defines the volume $V$ occupied by the hydrocarbon chains. The local micelle structure thus changes continuously from cylindrical micelle at the circular base of each pyramid to planar bilayer at the midpoint D of the junction. A straightforward geometrical analysis of this model yields
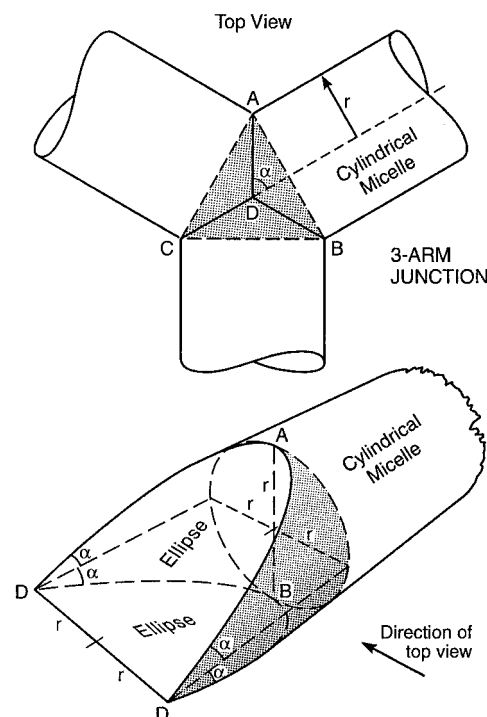
(22) Gorski, N.; Kalus, J.; Kuklin, A. I.; Smirnov, L. S. *J. Appl. Crystallogr.* **1997**, *30*, 739.

(23) Only the first Bragg reflection of the hexagonal lattice was measured because the physical dimensions of the SANS pressure cell precluded access to higher *q* values.

(24) Tlusty, T.; Safran S. A.; Strey, R. *Phys. Rev. Lett.* **2000**, *84*, 1244.



**Figure 3.** Three-arm junction model.

$$A = \frac{2(\pi - 2)r^2}{\tan \alpha} \tag{2}$$

and

$$V = \frac{2\left(\pi - \frac{4}{3}\right)r^3}{\tan \alpha}$$

per arm, which gives $\eta = 0.79 r/l_c$. Similarly, $\eta = 0.50 r/l_c$ for cylinders. The maximum value of $\eta$ for a particular micelle geometry is determined by the constraint that surfactant molecules can no longer pack into that geometry when $r > l_c$. Therefore, as $\eta$ approaches then exceeds 0.5, we expect cylindrical micelles first to grow in length to minimize their increasingly unfavorable spherical end caps and then to form junctions that effectively replace the highly unfavorable spherical end caps by energetically favorable junctions. Since the cylinders and junctions can coexist for $\eta < 0.5$, we write

$$\eta = [0.50(1 - \phi_{junc}) + 0.79\phi_{junc}](r/l_c) \leq 0.5 \tag{3}$$

where $\phi_{junc}$ is the fraction of surfactant molecules in the junctions.[25] This expression relates $\phi_{junc}$ to $\eta$ for a given value of $r$.

Using the cylindrical radius of 21 Å obtained from our SANS experiments, $r \approx 10.5$ Å, since we are interested in only that "half" of the surfactant molecule corresponding to the hydrophobic tail. To calculate $\eta$, we set $l_c = 16.7$ Å for $C_{12}E_5$,[26] and $a_0 = 58$ Å$^2$ for $C_{12}E_5$/water solutions at 20 °C and ambient pressure.[27,28] We take $a_0$ to be independent

(25) Equation 3 follows directly from the assumption that the total hydrophobic core volume for a system of cylinders and junctions is simply $nv = n_{junc}v_{junc} + n_{cyl}v_{cyl}$, where $n$ is the total number of surfactant molecules and $n_i$ is the number of surfactant molecules in the junctions ($i = $ junc) and the cylinders ($i = $ cyl).

(26) Tanford, C. *The Hydrophobic Effect: Formation of Micelles and Biological Membranes*; John Wiley & Sons: New York, 1980.

(27) Strey, R.; Glatter, O.; Schubert, K.-V.; Kaler, E. W. *J. Chem. Phys.* **1996**, *105*, 1175.
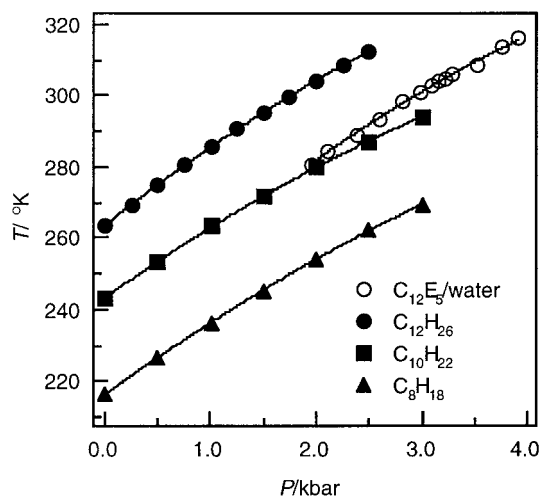
**Figure 4.** Pressure–temperature curves for the $L_1 \rightarrow H_1$ phase transition for a 1 wt % $C_{12}E_5$/water solution, and the freezing transitions for pure *n*-octane (Würflinger, A. *Ber. Bunsen-Ges. Phys. Chem.* **1975**, *79*, 1195), *n*-decane (Würflinger, A. *Ber. Bunsen-Ges. Phys. Chem.* **1975**, *79*, 1195), and *n*-dodecane. (Landau, R.; Würflinger, A. *Ber. Bunsen-Ges. Phys. Chem.* **1980**, *84*, 896). (The lines are drawn to guide the eye.)

of pressure. Finally, measurements of $C_{12}E_{n\geq6}$/water solution densities at 25 °C and pressures up to 1500 bar show that the volume per oxyethylene group remains constant while the micelle hydrophobic core is compressed with increasing pressure.[29] The pressure dependence of the hydrophobic core volume per surfactant molecule is given by $v = 387[1 - (7.7 \times 10^{-5})(P - 1)]$ Å$^3$, with the pressure in bar.[29] At ambient pressure and 20 °C, we calculate $\eta = 0.40$, which gives $\phi_{\text{junc}} \sim 0.47$. Both $v$ and $\phi_{\text{junc}}$ decrease with increasing pressure, from which we conclude that the formation of three-arm junctions becomes increasingly unfavorable at higher pressures due to the compression of the $C_{12}E_5$ micelle hydrophobic core. Moreover, $\phi_{\text{junc}} = 0$ at ~2750 bar and 20 °C, which is in good agreement with our observation of a transition between 2410 and 2550 bar at this temperature.

If we assume the $C_{12}E_5$ micelle hydrophobic core to be a pure liquid *n*-alkane, then it follows that compression of the core would eventually lead to its solidification as the result of a pressure-induced freezing transition. In Figure 4, the temperature dependence of the transition pressure is compared to the $p$–$T$ freezing curves for pure *n*-octane, *n*-decane, and *n*-dodecane. This $p$–$T$ curve was determined experimentally by visual observation and is identical to the $p$–$T$ curve obtained previously by others for the same $C_{12}E_5$/water solution and for a pressure-induced transition in which solid precipitates from a clear micellar solution to form macroscopic aggregates.[12] The $p$–$T$ curve for the $C_{12}E_5$/water solution in Figure 4 runs parallel to the $p$–$T$ curve for *n*-dodecane but is shifted to higher pressures, as one would expect given the destabilizing influence of the surfactant headgroup on the

hydrocarbon chain. The freezing point depression at constant pressure that corresponds to this shift is ~22 °C, which is reasonable for *n*-dodecane confined within a cylindrical micelle core of this diameter.[30] If we take the $C_{12}E_5$ micelle hydrophobic core to be *n*-decane, then we would expect the core to freeze at a pressure of ~2500 bar at 20 °C, which is close to the pressure for the $L_1 \rightarrow H_1$ phase transition at this temperature. We propose, therefore, that the hydrophobic core of the $C_{12}E_5$ micelle does freeze to form an amorphous solid at these conditions, such that the micelles lose flexibility and hence conformational entropy. The formation of hexagonally ordered bundles of cylindrical micelles follows as attractive van der Waals forces between the micelles are not offset by the loss of repulsive undulation forces arising from the fluidity of the hydrophobic core.

The stability of this ordered hexagonal microstructure at high pressures can be estimated from the Lindemann criterion for melting a hexagonal lattice of purely repulsive, thermally undulating cylinders. This criterion specifies that the hexagonal lattice melts when the root-mean-square undulation amplitude exceeds a certain fraction of the interaxial spacing between cylinders; specifically, the lattice constant has a maximum value on the order of ~1.2 times the diameter of the cylinders at the melting point.[31,32] A factor slightly larger than 1.2 is expected for $C_{12}E_5$ micelles due to attractive intermicelle interactions that would further stabilize the hexagonal lattice. From our SANS data at 20 °C, the lattice constant is $a = 4\pi/q\sqrt{3} = 59.4$ Å in the $H_1$ phase at ambient pressure, and $a = 55.8$ Å in the new high-pressure phase at 2550 bar. The diameter of the cylindrical micelles is taken to be $b = 42.0$ Å at all pressures. For the $H_1$ phase at ambient pressure, therefore, $a \approx 1.4b$, which clearly corresponds to a stable hexagonal lattice of cylindrical micelles. At 2550 bar, we find $a \approx 1.3b$, thus indicating that hexagonally ordered bundles of $C_{12}E_5$ cylindrical micelles are indeed stable at this higher pressure as well. As the pressure is lowered, however, entropic repulsive forces between the cylindrical micelles are restored, the lattice spacing increases in response to these forces, and the bundles melt to form a network of semiflexible, cylindrical micelles. Interestingly, undulation forces may be implicated in a similar transition from a network of semiflexible, cylindrical micelles to ordered bundles of cylindrical micelles observed during the template-mediated polymerization of the counterion for cetyltrimethylammonium 4-vinylbenzoate micelles.[33]

(28) Brunner-Popela, J.; Mittelbach, R.; Strey, R.; Schubert, K.-V.; Kaler, E. W.; Glatter, O. *J. Chem. Phys.* **1999**, *110*, 10623.
(29) Kaneshina, S.; Yoshimoto, M.; Kobayashi, H.; Nishikido, N.; Sugihara, G.; Tanaka, M. *J. Colloid Interface Sci.* **1980**, *73*, 124.

(30) Jackson, C. L.; McKenna, G. B. *J. Chem. Phys.* **1990**, *93*, 9002.
(31) Selinger, J. V.; Bruinsma, R. F. *Phys. Rev. A* **1991**, *43*, 2910.
(32) Roux, D.; Coulon, C. *J. Phys. (Paris)* **1986**, *47*, 1257.
(33) Kline, S. R. *Langmuir* **1999**, *15*, 2726.